

Electronic and magnetic properties of the Ti_5O_9 Magnéli phase

I. Slipukhina* and M. Ležaić

Peter Grünberg Institut and Institute for Advanced Simulation, Forschungszentrum Jülich and JARA, D-52425 Jülich, Germany

(Received 6 August 2014; revised manuscript received 7 October 2014; published 30 October 2014)

Structural, electronic, and magnetic properties of Ti_5O_9 have been studied by *ab initio* methods in low-, intermediate-, and high-temperature phases. We have found the charge and orbital order in all three phases to be nonunique, and the formation of Ti^{3+} - Ti^{3+} bipolaronic states less likely as compared to Ti_4O_7 . Several quasidegenerate magnetic configurations were calculated to have different width of the band gap, suggesting that the reordering of the unpaired spins at Ti^{3+} ions might at least partially be responsible for the changes in conductivity of this material.

DOI: [10.1103/PhysRevB.90.155133](https://doi.org/10.1103/PhysRevB.90.155133)

PACS number(s): 31.15.A–, 71.20.–b, 75.25.Dk

I. INTRODUCTION

For several decades binary transition-metal oxides and related compounds have attracted increasing attention as resistive-switching materials. These are materials which can be switched between a high- and a low-resistance state and are very promising candidates for the next-generation nonvolatile resistive random access memory (RRAM). The resistive switching in many of these technologically relevant oxides is claimed to be based on the formation and disruption of highly conductive filaments, through which the current flow is realized. However, still very little is known about the composition, structure, and dimensions of these filaments.

Recent low-temperature conductivity and *in situ* current-voltage measurements confirmed that the conducting filaments in Pt/ TiO_2 /Pt [1], as well as Fe-doped SrTiO_3 [2], are composed of Ti_4O_7 and Ti_5O_9 Magnéli phases and their mixtures. These compounds belong to the homologous series $\text{Ti}_n\text{O}_{2n-1}$ ($3 \leq n \leq 9$) of Ti oxides with TiO_2 and Ti_2O_3 as the end members. Structurally they are related to rutile: there are adjacent rutile-like chains of n edge-sharing TiO_6 octahedra, running parallel to the pseudorutile c_R axis (see Fig. 1); the octahedra at the end of each of the chains share their faces with the next pseudorutile chain. With the exception of Ti_2O_3 , these compounds possess a triclinic structure and they are mixed-valence compounds with two Ti^{3+} ($3d^1$ electronic configuration) and $(n - 2)$ Ti^{4+} ($3d^0$) ions per formula unit (in an ionic picture). Several members of this homologous series, as well as the isostructural vanadium Magnéli phases $\text{V}_n\text{O}_{2n-1}$, are known to exhibit phase transitions with temperature, at which their conductivity changes drastically (it is the largest for $n = 3, 4$, and 5 and reduces for the members with higher n). These transitions were interpreted in terms of the localization of the electrons in the cation sublattice. Indeed, the presence of both Ti^{3+} and Ti^{4+} ions provides several possibilities of charge distribution at cation sites, resulting in various charge-ordered states.

Take Ti_4O_7 for example, which undergoes two consecutive phase transitions with temperature: a semiconductor-semiconductor transition at 130 K and a semiconductor-metal transition at 150 K [3]. X-ray diffraction studies [4] on Ti_4O_7 single crystals revealed that at low temperatures Ti^{3+} ions are

covalently bonded to form the so-called *bipolarons*—singlet electron pairs (Ti^{3+} - Ti^{3+} pairs). In the low-temperature (LT) semiconducting phase these pairs order so that they occupy alternate pseudorutile chains. In the high-temperature (HT) phase the pairing is believed to be absent and all the Ti cations are in the same oxidation state $\text{Ti}^{3.5+}$, resulting in further increase of the conductivity and metallic behavior. The nature of the intermediate temperature (IT) phase remains rather unclear; however it is commonly believed that the (semiconductor-semiconductor) transition from LT to IT phase is accompanied by the reordering of the Ti^{3+} - Ti^{3+} pairs [4]. It was assumed that in the IT phase bipolarons distribute in Ti chains with a long-range order that requires a fivefold superstructure (bipolaron liquid state [5]). Later, the structure of the IT phase was revisited and suggested to be more complicated with the presence of bipolarons and a long-range order of Ti valences [6]. Recent photoemission experiments [7] interpreted the IT phase in Ti_4O_7 as a highly anomalous state sandwiched between the mixed-valent Fermi liquid (HT phase) and charge-ordered Mott-insulating phase (LT phase).

Two distinct phase transitions were also observed in Ti_5O_9 , at 128 K and 139 K, accompanied by the conductivity decrease by a factor of 3 (Ref. [8]) (or 50 according to Bartolomev and Frankl [9]). While LT and IT phases are found to be semiconducting, the conductivity in the HT phase increases with increasing temperature, which means that this phase is not a true metal and its nature is not clear. Compared to Ti_4O_7 , for which a stable charge-ordered state was shown to exist at low temperature, the charge order in Ti_5O_9 is rather uncertain, since the number of Ti ions in the pseudorutile chains is odd, preventing the formation of the Ti^{3+} long-range ordered pairs. X-ray studies performed by Marezio *et al.* [8] did not reveal any localization of charges and/or formation of covalent bonds between the Ti^{3+} cations in Ti_5O_9 . However, in order to explain the semiconducting properties of the LT and IT phases, which in Ti_4O_7 are related to the formation of Ti^{3+} - Ti^{3+} pairs, they suggested a microdomain structure of the material with Ti^{3+} mostly present at domain walls, making the detection of the charge localization and Ti^{3+} - Ti^{3+} bond formation by x-ray techniques rather impossible. The authors associated the observed EPR (electron paramagnetic resonance) signal with the presence of unpaired Ti^{3+} . Watanabe [10] has recently studied the structural changes across the phase transitions in Magnéli phases by means of Raman spectroscopy. He observed two semiconductor-semiconductor transitions, at 137 K and

*Corresponding author: i.slipukhina@fz-juelich.de

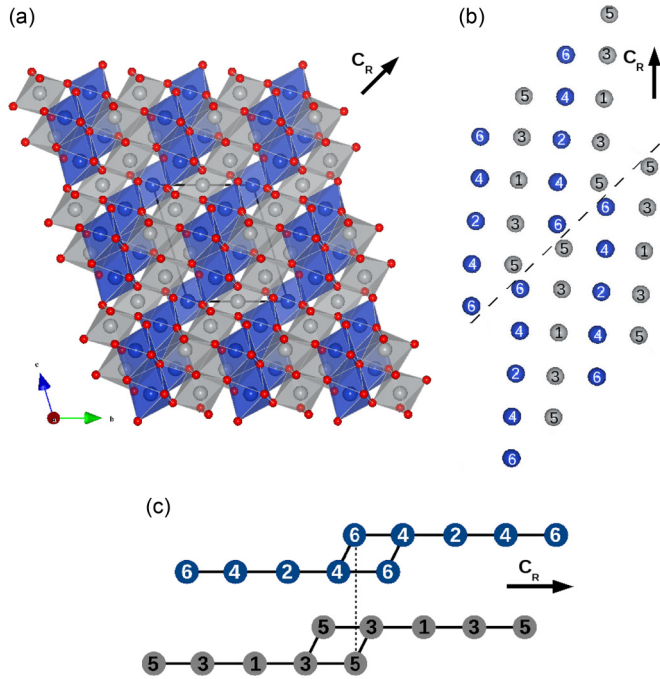


FIG. 1. (Color online) The crystal structure of Ti_5O_9 : spatial view (a), schematic view of the chain structure (b), and two adjacent Ti chains (c). The Ti atoms in the adjacent chains, which run parallel to the pseudorutile c_R axis, are shown in gray and blue, while oxygen atoms are shown in red. The black dashed line indicates the shear plane.

130 K, and revealed a fine structure of the LT phase, somewhat resembling the IT phase of Ti_4O_7 . He suggested a considerable disorder for the LT phase of Ti_5O_9 and a rather itinerant nature of the $3d$ electrons in the IT and HT phases as in the HT phase of Ti_4O_7 . The author did not observe any clear tendency as to the nature of the charge ordering in the considered Magnéli phases and concluded that in the compounds with odd n like Ti_5O_9 the charge order is unstable.

The effect of pressure on the phase transitions in $\text{Ti}_n\text{O}_{2n-1}$ ($n = 4, 5, 6$) Magnéli phases was studied in Ref. [11]. In contrast to a commonly accepted bipolaronic picture of the metal-insulator transition in these compounds, which is attributed to the strong electron-lattice coupling, the authors proposed their own explanations of the physics behind the phase transitions. The remarkably enhanced pressure effect on the phase transition temperatures as n goes from 6 to 4 the authors explained by a delicate interplay between the electron-lattice coupling and electron correlations. In this respect charge ordering in Ti_4O_7 is explained to be due to dominant electron correlations with a subsequent bipolaron formation by an electron-lattice coupling. Ti_6O_{11} , on the contrary, is believed to be a small polaron insulator due to a prevailing electron-lattice coupling. Ti_5O_9 is suggested to be in between these two extreme cases. The formation of small polarons, localized on one atomic site and randomly distributed over the lattice, explains rather well the unclear charge distribution in higher n Magnéli phases, observed in earlier experimental works [8,12]. The substantial Curie contribution, observed in Ti_5O_9 at low temperatures [13], which can be associated with

the presence of unpaired localized moments, is also in line with the proposed small-polaron picture. A distinct pressure dependence of the resistivity in the HT phase of Ti_5O_9 allowed the authors to assume that the system is just at the crossover region from large to small polarons. Such crossover in the systems with intermediate electron coupling is often associated with a metal-insulator transition.

As for the magnetic properties, Ti_5O_9 as well as Ti_4O_7 and Ti_6O_{11} phases show antiferromagnetic (AFM) behavior with Néel temperature (T_N) of about 130 K [14]. According to magnetic susceptibility measurements in Ti_5O_9 , there are two transitions which occur at 128 and 138 K, in contrast to Ti_4O_7 with only one transition in magnetic susceptibility. The T_N is very close to the phase transition temperature, which allows one to relate the magnetic ordering with the phase transitions observed in this compound. At low temperatures ($T < 40$ K) the measurements show a Curie behavior, while for the $40 \text{ K} < T < 128 \text{ K}$ the temperature-independent susceptibility might be due to Van Vleck paramagnetism. Susceptibility in the HT phase is clearly temperature independent. Based on the measured molar susceptibility in Ti oxides, the effective magnetic moment for Ti_5O_9 was calculated to be of $0.245 \mu_B$ and it was concluded that a relatively small percentage of the unpaired electrons (7.4%) contributes to the Curie-Weiss behavior, while a large percentage (92.6%) contributes to its metallic (free electron gas) behavior; the small Weiss constant indicates that these spins do not interact strongly [15].

Although rather well studied experimentally, there is very little known about the mechanism behind the transitions in Magnéli phases theoretically. Up to today, there are only a few DFT calculations on Ti_4O_7 [16–20], and to our knowledge, they are completely lacking for higher- n phases. Therefore, in this work we aimed to develop a fundamental understanding of the mechanisms that underlie the phase transitions in Magnéli phases like Ti_5O_9 , which, due to its high electrical conductivity and chemical stability, has a promising application not only in electrochemical engineering, but even in medicine as a neural stimulation electrode [21]. With this aim we performed DFT calculations in order to illuminate the changes in its electronic structure on a microscopic level and establish relations between the structural, electronic, and magnetic properties and their implications for conductive phenomena. We believe that the obtained results will be helpful in interpreting the physics of resistively switching Ti oxides.

II. COMPUTATIONAL DETAILS

The electronic and magnetic properties of the different phases of Ti_5O_9 were studied within the DFT, using the Vienna *ab initio* Simulation Package (VASP) [22,23] with projector augmented potentials (PAW) [24,25]. A kinetic energy cutoff of 450 eV and a $6 \times 6 \times 6$ \mathbf{k} -point mesh was used for the unit cell of 28 atoms. The exchange correlation functional was treated within the generalized gradient approximation (GGA) [26,27]. The GGA + U approximation in Dudarev's approach [28] with U applied to $3d$ states of Ti was used to take into account the electronic correlations.

The structural data for all three phases have been taken from Ref. [8]. The structure optimization was performed only for the LT phase with the aim to find the ground state of the

system under study. For the sake of simplicity, we do not consider the spin-orbit coupling in our calculations, and we restrict ourselves to the collinear spins only.

III. RESULTS AND DISCUSSION

A. Correlation effects

It is known that oxygen-deficient rutile TiO_{2-x} can be transformed into a Magnéli phase, when oxygen nonstoichiometry is sufficiently high ($x > 0.001$ [29]). At such concentrations, oxygen vacancies arrange into extended defects, resulting in the shear plane structure [see Fig. 1(c)]. As a result, the defect states appear in the band gap close to the conduction band minimum, which are occupied by the electrons of Ti^{3+} ions. Numerous studies on TiO_{2-x} , including recent hybrid functional calculations [30], have reported on the effect of the electronic correlations on the position of these defect states and the distribution of Ti^{3+} ions. For Ti_4O_7 or Ti_5O_9 with similar peculiarities of the electronic structure, the $+U$ approach or hybrid functionals were used to correctly account for the correlation effects and were able to reproduce the ground-state properties of the phases [16–20]. However, the correlations might be less effective in the phases with larger n (i.e., with smaller density of $3d$ electrons), as was assumed in Ref. [10] based on the observed lack of the systematic trend in charge ordering in different Magnéli phases.

In order to elucidate the importance of electron correlations for the charge localization in Ti_5O_9 , we have performed calculations within the GGA $+U$ approach, assuming the unit-cell model for the order/disorder of the Ti^{3+} and Ti^{4+} ions. To cover the limits of weak and strong electron interactions, the on-site Coulomb energy parameter was varied within the range $0 < U < 6$ eV. The evolution of the density of electronic states (DOS) with U in the LT phase with the experimental structure is presented in Fig. 2; these calculations were performed assuming an AFM spin coupling with a zero total magnetic moment per cell.

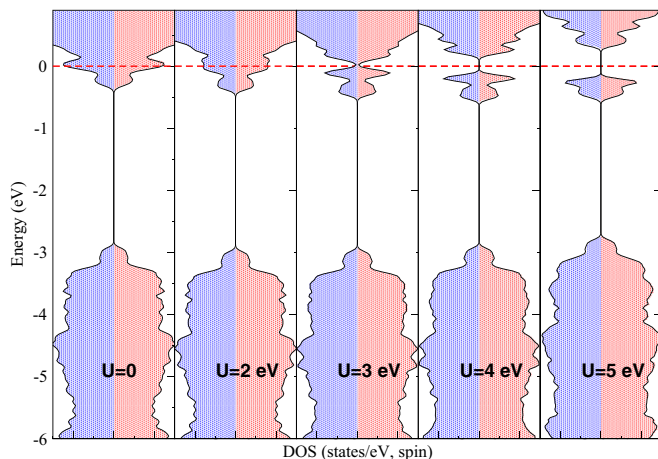


FIG. 2. (Color online) The GGA $+U$ spin-polarized DOS, calculated for the LT phase of Ti_5O_9 at different U for the AFM spin alignment. The Fermi level is at zero energy (shown by red dashed line). Blue and red shading denotes the majority and minority spins, correspondingly.

TABLE I. The GGA $+U$ absolute values of magnetic moments $|M|$ (in μ_B) at Ti sites in the LT phase of Ti_5O_9 , calculated for different U (at $J = 1$ eV) for the AFM/FM spin alignment. The energy gaps E_g (in eV) and the total energy differences $\Delta E = E_{\text{AFM}} - E_{\text{FM}}$ (in meV/f.u.) are also listed.

	$U = 2$ eV	$U = 3$ eV	$U = 4$ eV	$U = 5$ eV	$U = 6$ eV
Ti(1)	0/0.21	0/0.23	0/0.15	0/0.14	0/0
Ti(2)	0/0.47	0/0.52	0/0.50	0/0.55	0/0.44
Ti(3)	0.29/0.30	0.37/0.43	0.38/0.45	0.28/0.44	0/0.56
Ti(4)	0.19/0.30	0.43/0.36	0.58/0.43	0.71/0.37	0.81/0.43
Ti(5)	0.27/0.19	0.32/0.47	0.37/0.49	0.53/0.61	0.77/0.59
Ti(6)	0/0.09	0/0.26	0/0.22	0/0.17	0/0.12
E_g	0/0	0/0	0.1/0	0.4/0	0.7/0
ΔE	55	47	23	-19	-72

As follows from Fig. 2, for $U \leq 3$ eV the DOS remains metallic with Ti $3d$ states merged into the conduction band. A small band gap of about 0.1 eV between the occupied and unoccupied $3d$ states of Ti opens in both spin channels at $U > 3$ eV, and it increases up to 0.7 eV at $U = 6$ eV (see Table I). It should be noted that an energy gap of 0.7 eV was also obtained for Ti_4O_7 at $U = 0.4$ Ry (5.4 eV) in Ref. [19] (the choice of this value of U was justified by comparing the total energy difference between the three phases at different U with the transition temperatures). The topology of the insulating DOS very much resembles that of the Ti_4O_7 [17–19]. The well-localized states just below the Fermi level are formed by the $3d$ orbitals of Ti possessing nonzero magnetic moment. Figure 3 shows the spatial distribution of these localized gap states, calculated at $U = 6$ eV. It is clear that the system is not only charge ordered, but also orbitally ordered: occupied orbitals at different Ti^{3+} sites are of d_{xy} and d_{xz} (or d_{yz}) symmetry, if we define them in the local frame of the octahedra. While the conduction band is mainly contributed by Ti $3d$ states, the valence band originates from the oxygen $2p$ states

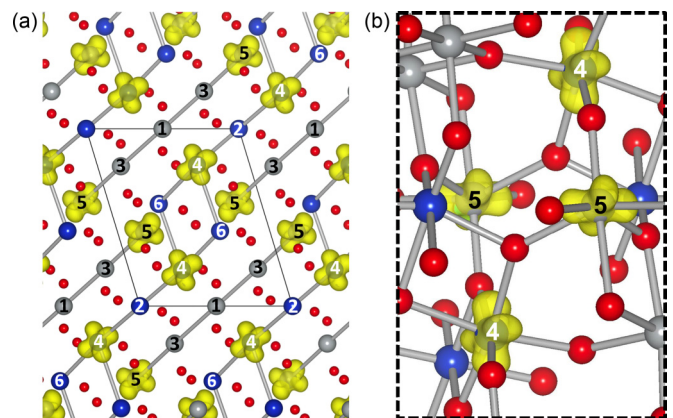


FIG. 3. (Color online) $3d$ valence charge distribution in the LT phase of Ti_5O_9 : (a) general view with Ti-Ti bonds; (b) zoomed view with Ti-O bonds. The calculated charge density isosurfaces correspond to the Ti^{3+} gap states. The presented results were obtained at $U = 6$ eV for the AFM spin configuration with $M_{\text{tot}} = 0$. Blue and gray colors distinguish between the Ti atoms in the adjacent pseudorutile chains. Note different orientation of the t_{2g} -like orbitals.

(with a small admixture of Ti $3d$ states due to Ti-O bond formation) and it is separated from the gap states by an energy interval, which is much larger than the fundamental gap. This gap decreases with the increasing U from around 2.8 eV at $U = 0$ to 1.9 eV at $U = 6$ eV. The width of the split-off $3d$ band is decreasing as the electron localization increases with the increased U . Following the evolution of the DOS as a function of U parameter, it is difficult to make certain conclusions on the appropriate value of U in the case of Ti_5O_9 , since the existing experimental data about the electronic band structure of Ti Magnéli phases is quite diverse. According to Mulay *et al.* [13], who studied the cooperative magnetic transitions in titanium oxides, the band gap of Ti_5O_9 in the LT phase is found to be of 0.035 eV. The authors also report on the gap of 0.041 eV for Ti_4O_7 , while optical measurements in Ref. [31] gave a band gap of 0.25 eV; later photoemission spectroscopy experiments revealed a gap of only 0.1 eV [7]. One is clear: even if the electron-electron interactions are less pronounced in Ti_5O_9 than in the other Magnéli phases with higher concentration of $3d$ electrons, they play an important role in the stabilization of its insulating ground state.

B. Structural effects

As mentioned earlier, Ti_5O_9 crystallizes in the triclinic $P\bar{1}$ structure with two formula units per unit cell. There are six crystallographically independent Ti atoms in its unit cell, surrounded by distorted oxygen octahedra (see Fig. 1 and Table II). These atoms form two crystallographically independent pseudorutile chains: Ti(5)–Ti(3)–Ti(1)–Ti(3)–Ti(5) and Ti(6)–Ti(4)–Ti(2)–Ti(4)–Ti(6) [32]. Among them Ti(1) and Ti(2) are at the center of symmetry, and Ti(5) and Ti(6) atoms are the nearest to the shear planes and their environment is not rutile-, but sesquioxide-like, similarly to the Ti_4O_7 . The Ti(5)–Ti(6) distance is ~ 2.83 Å and is the shortest in the lattice (see Table III). The oxygen octahedra around these atoms are severely distorted (the difference in Ti-O distances is ~ 0.3 Å) (see Table II). According to Ref. [8],

TABLE II. Ti-O interatomic distances (in Å) in the LT (115 K) and HT (295 K) phases of Ti_5O_9 according to structural parameters from Ref. [8].

	115 K	295 K		115 K	295 K
Ti(1)–O(2)	1.949	1.955	Ti(4)–O(5)	1.978	1.987
Ti(1)–O(3)	1.963	1.970	Ti(4)–O(6)	2.085	2.095
Ti(1)–O(4)	2.009	2.015	Ti(4)–O(9)	2.086	2.092
Ti(2)–O(1)	2.013	2.008	Ti(5)–O(5)	1.849	1.842
Ti(2)–O(2)	1.973	1.974	Ti(5)–O(6)	2.055	2.053
Ti(2)–O(5)	2.004	2.007	Ti(5)–O(7)	2.145	2.155
Ti(3)–O(1)	1.903	1.906	Ti(5)–O(7)	2.002	1.992
Ti(3)–O(2)	1.939	1.929	Ti(5)–O(8)	1.956	1.943
Ti(3)–O(3)	1.991	1.976	Ti(5)–O(9)	2.045	2.040
Ti(3)–O(6)	2.029	2.035	Ti(6)–O(4)	1.879	1.883
Ti(3)–O(7)	2.075	2.071	Ti(6)–O(6)	2.143	2.133
Ti(3)–O(8)	2.081	2.086	Ti(6)–O(7)	1.991	2.003
Ti(4)–O(1)	1.942	1.943	Ti(6)–O(8)	1.855	1.856
Ti(4)–O(3)	1.902	1.907	Ti(6)–O(9)	2.196	2.186
Ti(4)–O(4)	2.007	1.995	Ti(6)–O(9)	1.976	1.981

TABLE III. Ti-Ti interatomic distances (in Å) in the LT (115 K), IT (135 K), and HT (295 K) phases of Ti_5O_9 according to structural parameters from Ref. [8].

	115 K	135 K	295 K
Ti(1)–Ti(3)	2.930	2.932	2.928
Ti(2)–Ti(4)	2.906	2.908	2.924
Ti(3)–Ti(5)	2.979	2.989	3.004
Ti(4)–Ti(6)	3.037	3.043	3.041
Ti(5)–Ti(6)	2.827	2.816	2.829

the Ti(5)–Ti(3)–Ti(1)–Ti(3)–Ti(5) chains are more distorted than the Ti(6)–Ti(4)–Ti(2)–Ti(4)–Ti(6) one, and thus have a slightly larger separation of charge. However, as can be seen from Table III, these distortions are very small and structurally the low-temperature phases are almost identical to the HT phase. This is not the case for Ti_4O_7 , where the formation of bipolarons in the LT phase and their rearrangement into polarons and bipolarons in the IT phase with the consequent collapse in the HT phase are clearly related to the electron-lattice coupling. The transition from HT to LT phase in Ti_4O_7 is accompanied by an essential decrease in the Ti-Ti distances (~ 0.2 Å) with a consequent charge localization at Ti ions, involved in longer Ti-O and shorter Ti-Ti bonds. Interestingly, in the isostructural V_4O_7 no changes in cation-cation distances larger than ~ 0.06 Å are observed at the phase transition, despite the clear separation of charge into V^{3+} and V^{4+} in the alternate chains. Similar behavior applies to another member of the vanadium series, V_5O_9 , which undergoes a metal-insulator transition at 135 K [32]. Although incomplete, V-V dimerization is clearly observed in V_4O_7 [33], while it is negligible in V_5O_9 [34]. It was speculated that there are many different bonding patterns in the latter two compounds, and that an average of these patterns is observed by the classical x-ray diffraction methods [32].

Obviously, if the insulating behavior was induced by the lattice distortions only, the crystalline symmetry below the phase transition would be lower than in the metallic region. However, this is not the case in the Ti_5O_9 crystal, although its LT phase is slightly more distorted than the HT one. To find out how these small lattice distortions at the phase transitions affect the electronic properties of Ti_5O_9 , we performed total-energy calculations for the experimental structures [8] of all three phases. Figure 4 shows the density of states (DOS) of Ti_5O_9 , calculated at $U = 5$ eV for the LT, IT, and HT structures (as reported by Marezio *et al.* [8]), assuming an AFM spin ordering with zero total moment per cell. One can clearly see that the DOSs for all three phases are very similar to each other. They all are insulating with the band gap in the LT phase of about 0.43 eV and only slightly smaller gap of 0.38 eV in the IT and HT phases. The corresponding charge distribution is similar from phase to phase with only a slight difference in the Ti magnetic moments (see Tables IV and V for $M_{\text{tot}} = 0$). Therefore, although the peculiarities of the crystalline structure of Ti_5O_9 are certainly reflected in the rich variety of the possible charge order patterns, the lattice distortions at the phase transitions are rather insignificant to have a crucial effect on the conducting properties of the material.

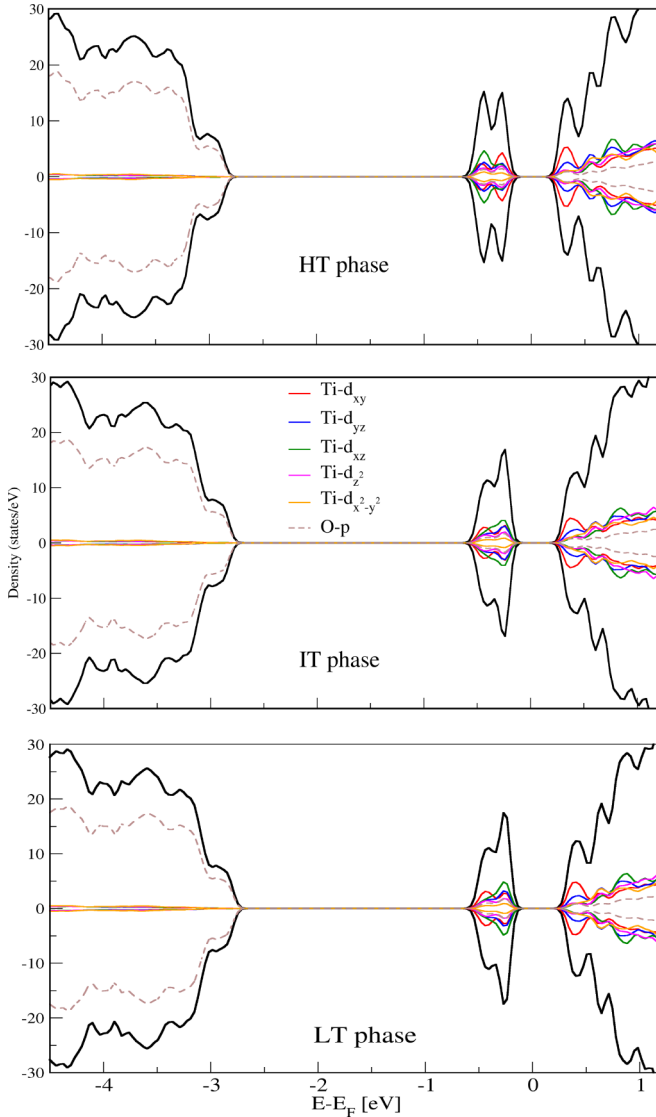


FIG. 4. (Color online) The GGA + U spin-polarized density of electronic states (DOS), calculated for the LT, IT, and HT phases of Ti_5O_9 at $U = 5$ for the AFM spin alignment (the lowest-energy configuration in Fig. 5). Positive (negative) values indicate spin-up (spin-down) DOS.

C. Magnetic and charge order

To find the ground-state magnetic ordering and which Ti atoms participate in it, we have considered an antiferromagnetic and a ferromagnetic (FM) spin configuration along with a nonmagnetic one (which turned out to be much higher in energy for all three phases). First, we have considered the effect of electron correlations on the magnetic behavior of the crystal. For the experimental structures we have found that at $U \leq 4$ eV the LT phase is FM and metallic, while for larger U it tends to be an AFM insulator (see Table I). Depending on the chosen U and the resulting spin configuration, the calculated magnetic moments on each of the inequivalent Ti atoms vary within the range $0.1\text{--}0.8 \mu_B$. This is in contrast to Ti_4O_7 , for which the ionic magnetic moments in the LT phase were calculated to be robust with respect to their relative orientation and thus were linked to the local

structure around Ti [19]. As follows from Table I, even in the FM state the magnetic moment is distributed among all the Ti atoms somewhat inhomogeneously. In the AFM state the charge disproportionation is more pronounced within the whole range of U values and a nonzero moment is observed only at the Ti(3), Ti(4), and Ti(5) sites. While Ti(4) and Ti(5) magnetic moments increase with increasing U , the moment at the Ti(3) site starts to decrease for $U > 4$ and is completely suppressed at $U = 6$ eV (nominal Ti^{3+} and Ti^{4+} ions become clearly distinguishable). When the Ti(3) moment becomes zero, the charge order pattern is symmetric with respect to the inversion. At the FM spin alignment the behavior is somewhat different: the charge order pattern is less symmetric, but more homogeneous, and it is less sensitive to the changes of U value. As a result, the energy gap is zero for the whole range of U values.

We have performed fixed spin moment calculations for all three phases by calculating the total energy at the constrained magnetic moment of the unit cell. The results, obtained for $U = 5$ eV, are presented in Table IV and Table V. We chose this value of U parameter, since this value was shown to give energy gaps compatible with experiment and hybrid functional calculations for other members of this family of compounds, in particular Ti_2O_3 and Ti_4O_7 [19,20]. It is clear from the listed data that there are several stable magnetic configurations with a very small relative energy difference, namely the configurations with total moment of 0 (AFM), 2, and $4 \mu_B/\text{cell}$. Moreover, for each of the magnetic configurations we have obtained a whole set of different possible charge order patterns (see Fig. 5); therefore, we present here only those which in our calculations have the lowest energy.

1. Low-temperature phase

For the experimental structure of the LT phase the configuration with the total magnetic moment $M_{\text{tot}} = 2\mu_B/\text{cell}$ is practically degenerate with the AFM configuration with $M_{\text{tot}} = 0$ (the energy difference is only 6 meV/f.u.) (see Table IV). The FM configuration with $M_{\text{tot}} = 4\mu_B/\text{cell}$ is 20 meV/f.u. higher in energy than the AFM one. We observe stronger localization of the charge, and hence, larger band gap, for the configurations where more Ti moments are aligned antiparallel to each other: the band gap is the largest for the AFM state and it decreases to zero for the FM one. Therefore, opening of the gap in Ti_5O_9 when going from high to low temperatures might be closely related with the AFM ordering of the unpaired spins. This is in line with the fact that experimentally the Néel temperature and the semiconductor-metal transition temperatures in this material nearly coincide.

Interestingly, as follows from Table IV, when structural relaxations are taken into account, the lowest energy charge distribution is the same for all three magnetic configurations. It is such that Ti^{3+} ions (polarons) are at the position of Ti(4) and Ti(5) cations. Within a pseudorutile chain they are well separated by either one or three Ti^{4+} ions (Fig. 3), retaining the inversion symmetry. While Ti^{3+} in the Ti(5) position has a common face with the Ti^{4+} at the Ti(6) site across the shear plane, the Ti^{3+} in the Ti(4) position is close to the middle of the pseudorutile chain. It is clear from Fig. 3(b) that there is no direct overlap between the t_{2g} orbitals at Ti(4) and Ti(5)

TABLE IV. Magnetic moments on Ti atoms (in μ_B), total energies ΔE with respect to the lowest-energy magnetic configuration (in meV/f.u.), and the band gap E_g (in eV), calculated for the experimental and relaxed (theoretical) structures of LT phase. The numbers in parentheses show the direction and magnitude of the magnetic moment of the crystallographically equivalent atoms in the unit cell in cases when they are not the same.

M_{tot}	$0\mu_B/\text{cell}$		$2\mu_B/\text{cell}$		$4\mu_B/\text{cell}$	
	Experimental	Relaxed	Experimental	Relaxed	Experimental	Relaxed
μ_{Ti}						
Ti(1)	0	0	0	0	0.14	0
Ti(2)	0	0	0.31	0	0.54	0
Ti(3)	-0.28(+0.28)	0	-0.17(+0.32)	0	0.44	0
Ti(4)	+0.71(-0.71)	+0.83(-0.83)	0.68	0.84	0.37	0.85
Ti(5)	-0.53(+0.53)	-0.81(+0.81)	-0.56(+0.56)	-0.80(+0.80)	0.61	0.84
Ti(6)	0	0	0	0	0.17	0
ΔE	6	0	0	2	26	7
E_g	0.46	0.9	0.19	0.82	0	0.67

sites and the interaction between the corresponding electrons is realized through the hopping via bridging oxygens.

Several decades ago, James and Catlow [35] theoretically predicted that the electrons created by the reduction of rutile or higher Magnéli phases should be trapped by the shear plane. In Ti_5O_9 this would result in a charge-ordered state with Ti^{3+} ions occupying Ti(5) and Ti(6) sites. However, in our calculations such state is ~ 148 meV/f.u. less stable than the lowest-energy one with Ti^{3+} at Ti(5) and Ti(4) sites. This means that not all electrons occupy the sites adjacent to the shear planes, but prefer the localization at the nearest-neighbor sites.

In contrast to the experimental structures, the localization of the charges in the relaxed structures is much stronger and it results in the insulating behavior even for the FM spin alignment. The total energy difference between the states with $M_{\text{tot}} = 0, 2,$ and $4\mu_B/\text{cell}$ is less than 10 meV/f.u. The fact that it is so small indicates that the charge and spin order are not unique. A large separation between the Ti^{3+} ions results in rather weak magnetic interactions, which is reflected in the small energy difference between the states with the same charge distribution, but different number of parallel/antiparallel spins. This is in line with the conclusions made by Danley and Muley [15], who observed a small Weiss constant and hence weak interaction between the unpaired spins in Ti_5O_9 . This is different from Ti_4O_7 , for which the AFM interaction between the spins within

the $\text{Ti}^{3+}\text{-Ti}^{3+}$ pairs was found to be rather strong [17], although the interpair coupling was calculated to be much weaker. We have also considered the states where four unpaired spins at Ti sites are distributed in the way to form bipolarons within the same pseudorutile chain, as well as the state with coexisting bipolarons and polarons. These states were obtained to be 11 meV/f.u. and 34 meV/f.u., correspondingly, higher in energy than the ground state and are both insulating. Therefore, the ground state of the LT phase of Ti_5O_9 is semiconducting; however its charge order pattern is not unique.

2. Intermediate- and high-temperature phases

Since our *ab initio* calculations are performed at $T = 0$ K temperature, for the IT and HT phases we have considered only the experimental structures as reported by Marezio *et al.* [8]. In analogy to the LT phase, we observe several stable magnetic configurations for the IT and HT phases, which are almost degenerate within our calculation error: these are the configurations with the total magnetic moment of 0, 2, and $4\mu_B/\text{cell}$. For each of these magnetic configurations our fixed-spin moment calculations revealed several possible charge-order patterns, but in Table V we present only the lowest-energy ones. For the IT phase the calculated band gap is the largest for the configuration with $M_{\text{tot}} = 0\mu_B/\text{cell}$ (about 0.4 eV) and

TABLE V. Magnetic moments on Ti atoms (in μ_B), ΔE total energies with respect to the lowest-energy magnetic configuration (in meV/f.u.), and the band gap E_g (in eV), calculated for the experimental structures of the IT and HT phases. The numbers in parentheses show the direction and magnitude of the magnetic moment of the crystallographically equivalent atoms in the unit cell in cases when they are not the same.

M_{tot}	$0\mu_B/\text{cell}$		$2\mu_B/\text{cell}$		$4\mu_B/\text{cell}$	
	IT	HT	IT	HT	IT	HT
μ_{Ti}						
Ti(1)	0	0	0	0	0.20	0
Ti(2)	0	0	0.35	0.27	0.68	0.29
Ti(3)	-0.25(+0.25)	-0.33(+0.33)	-0.13(+0.29)	-0.14(0.46)	0.43	0.41
Ti(4)	+0.71(-0.71)	+0.73(-0.73)	0.67	0.70	0.19	0.70
Ti(5)	-0.55(+0.55)	-0.46(+0.46)	-0.58(+0.57)	-0.56(0.39)	0.69	0.47
Ti(6)	0	0	0	0	0.19	0.14
ΔE	9	8	0	2	2	0
E_g	0.43	0.38	0.15	0.25	0	0.04

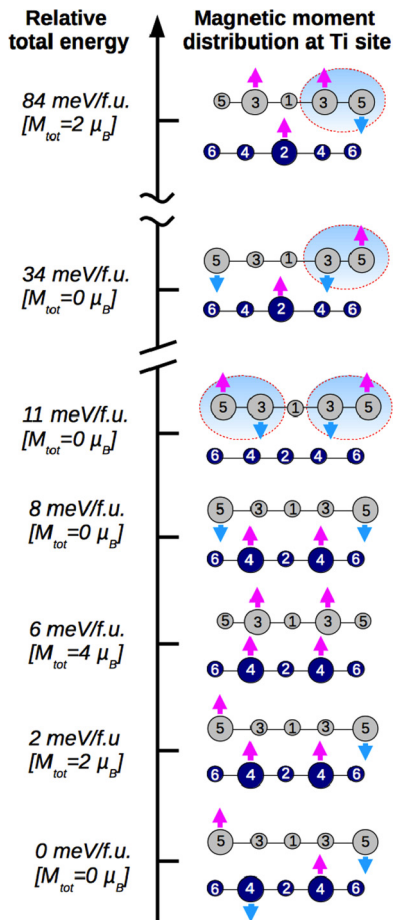


FIG. 5. (Color online) A schematic diagram showing the relative stability of several lowest-energy charge and magnetically ordered states, obtained for the LT phase taking into account structural relaxations. Shaded area within a red-dashed oval depicts Ti^{3+} - Ti^{3+} singlet pairs (bipolarons). Dark blue and gray colors are used to distinguish between Ti in adjacent pseudorutile chains. Big (small) balls denote Ti^{3+} (Ti^{4+}) ions.

it is almost the same as the gap calculated for the experimental structure of the LT phase. The gap is somewhat smaller for the configuration with $M_{\text{tot}} = 2\mu_B/\text{cell}$ and completely vanishes when the spins are aligned ferromagnetically due to more homogeneous distribution of the valence charge. Similar tendency is also observed for the HT phase with the only difference being that the gap (although very small) is nonzero for the FM configuration. It should be noted that for the HT phase there is another FM state, which is metallic and has a more homogeneous charge distribution, but this state is about 30 meV/f.u. higher in energy.

The magnetic moments do not vary much from phase to phase, which once again indicates a secondary role of the crystal structure in the electronic properties of the Ti_5O_9 . The charge distribution for the considered configurations resembles the one observed in the LT phase; however, it is slightly more localized for the FM configuration in the HT phase than in the LT or IT phases. However, the magnetic moment distribution remains inhomogeneous even for the FM configuration in the HT phase and does not correspond to the suggested $\text{Ti}^{3.5}$ picture. Therefore, the local environment and distortions play a visible role in the magnetic moment distribution in this material.

IV. CONCLUSIONS

In summary, we have performed first-principles calculations to study the electronic and magnetic properties of the Ti_5O_9 crystal, which belongs to the homologous series of $\text{Ti}_n\text{O}_{2n-1}$ oxides, known as Magnéli phases. From our results it is difficult to conclude which charge distribution is realized in this material at different temperatures, since for all three phases we find several quasidegenerate magnetic solutions. We therefore assume that the charge order within the cation sublattice in Ti_5O_9 is not unique, which makes its experimental detection at finite temperatures difficult. We suggest that in contrast to Ti_4O_7 , the formation of Ti^{3+} - Ti^{3+} pairs in this compound is less likely, although not completely impossible, since a bipolaronic state is only slightly higher in energy than the ground state. Our calculations performed for all three phases showed that crystal structure changes at the transitions make a minor influence on the electronic structure of the compounds. Although the electronic correlations are important for the stabilization of the insulating ground state, the phase transitions in this compound are related to a greater extent to a reordering of the unpaired spins. This conclusion agrees well with the antiferromagnetism model presented by Adler in Ref. [36], where the author considered different scenarios for the metal-nonmetal transitions in transition-metal oxides and sulfides. Thus, the mechanism behind the phase transitions in Ti_5O_9 must be a complex interrelation between the electronic correlations, electron-lattice, as well spin-lattice coupling.

ACKNOWLEDGMENT

We gratefully acknowledge funding from the Deutsche Forschungsgemeinschaft (DFG) within SFB 917 “Nanoswitches” and the Young Investigators Group Programme of the Helmholtz Association, Contract VH-NG-409, as well as the support of the Jülich Supercomputing Centre for computing time provided on supercomputer JUROPA (Project JIFF38).

[1] D.-H. Kwon, K. M. Kim, J. H. Jang, J. M. Jeon, M. H. Lee, G. H. Kim, X.-S. Li, G.-S. Park, B. Lee, S. Han, M. Kim, and C. S. Hwang, *Nat. Nanotechnol.* **5**, 148 (2010).

[2] R. Münstermann, T. Menke, R. Dittmann, and R. Waser, *Adv. Mater.* **22**, 4819 (2010).

[3] M. Marezio, D. B. McWhan, P. D. Dernier, and J. P. Remeika, *Phys. Rev. Lett.* **28**, 1390 (1972).

- [4] M. Marezio, D. B. McWhan, P. D. Dernier, and J. P. Remeika, *J. Solid State Chem.* **6**, 213 (1973).
- [5] S. Lakkis, C. Schlenker, B. K. Chakraverty, R. Buder, and M. Marezio, *Phys. Rev. B* **14**, 1429 (1976).
- [6] Y. Le Page and M. Marezio, *J. Solid State Chem.* **53**, 13 (1984).
- [7] M. Taguchi, A. Chainani, M. Matsunami, R. Eguchi, Y. Takata, M. Yabashi, K. Tamasaku, Y. Nishino, T. Ishikawa, S. Tsuda, S. Watanabe, C.-T. Chen, Y. Senba, H. Ohashi, K. Fujiwara, Y. Nakamura, H. Takagi, and S. Shin, *Phys. Rev. Lett.* **104**, 106401 (2010).
- [8] M. Marezio, D. Tranqui, S. Lakkis, and C. Schlenker, *Phys. Rev. B* **16**, 2811 (1977).
- [9] R. F. Bartolomew and D. R. Frankl, *Phys. Rev.* **187**, 828 (1969).
- [10] Masayuki Watanabe, *Phys. Stat. Sol. C* **6**, 260 (2009).
- [11] H. Ueda, K. Kitazawa, H. Takagi, and T. Matsumoto, *J. Phys. Soc. Jpn.* **71**, 1506 (2002).
- [12] Y. Le Page and P. Strobel, *J. Solid State Chem.* **47**, 6 (1983).
- [13] L. N. Mulay and W. J. Danley, *J. Appl. Phys.* **41**, 877 (1970).
- [14] L. K. Keys and L. N. Mulay, *Jpn. J. Appl. Phys.* **6**, 122 (1967).
- [15] W. J. Danley and L. N. Mulay, *Mater. Res. Bull.* **7**, 739 (1972).
- [16] V. Eyert, U. Schwingenschlögl, and U. Eckern, *Chem. Phys. Lett.* **390**, 151 (2004).
- [17] I. Leonov, A. N. Yaresko, V. N. Antonov, U. Schwingenschlögl, V. Eyert, and V. I. Anisimov, *J. Phys.: Condens. Matter* **18**, 10955 (2006).
- [18] L. Liborio, G. Mallia, and N. Harrison, *Phys. Rev. B* **79**, 245133 (2009).
- [19] M. Weissmann and R. Weht, *Phys. Rev. B* **84**, 144419 (2011).
- [20] A. C. M. Padilha, J. M. Osorio-Guillén, A. R. Rocha, and G. M. Dalpian, *Phys. Rev. B* **90**, 035213 (2014).
- [21] M. Canillas, E. Chinarro, M. Carballo-Vila, J. R. Juradoa, and B. Moreno, *J. Mater. Chem. B* **1**, 6459 (2013).
- [22] G. Kresse and J. Furthmüller, *Comput. Mater. Sci.* **6**, 15 (1996).
- [23] G. Kresse and J. Furthmüller, *Phys. Rev. B* **54**, 11169 (1996).
- [24] P. E. Blochl, *Phys. Rev. B* **50**, 17953 (1994).
- [25] G. Kresse and D. Joubert, *Phys. Rev. B* **59**, 1758 (1999).
- [26] J. P. Perdew, K. Burke, and M. Ernzerhof, *Phys. Rev. Lett.* **77**, 3865 (1996).
- [27] J. P. Perdew, K. Burke, and M. Ernzerhof, *Phys. Rev. Lett.* **78**, 1396 (1997).
- [28] S. L. Dudarev, G. A. Botton, S. Y. Savrasov, C. J. Humphreys, and A. P. Sutton, *Phys. Rev. B* **57**, 1505 (1998).
- [29] L. A. Bursil, B. G. Hyde, O. Terasaki, and D. Watanabe, *Philos. Mag.* **20**, 347 (1969).
- [30] A. Janotti, J. B. Varley, P. Rinke, N. Umezawa, G. Kresse, and C. G. Van de Walle, *Phys. Rev. B* **81**, 085212 (2010).
- [31] D. Kaplan, C. Schlenker, and J. J. Since, *Philos. Mag.* **36**, 1275 (1977).
- [32] M. Marezio, P. D. Dernier, D. B. McWhan, and S. Kachi, *J. Solid State Chem* **11**, 301 (1974).
- [33] A. S. Botana, V. Pardo, D. Baldomir, A. V. Ushakov, and D. I. Khomskii, *Phys. Rev. B* **84**, 115138 (2011).
- [34] M. Obara, A. Sekiyama, S. Imada, J. Yamaguchi, T. Miyamachi, T. Balashov, W. Wulfhekel, M. Yabashi, K. Tamasaku, A. Higashiya, T. Ishikawa, K. Fujiwara, H. Takagi, and S. Suga, *Phys. Rev. B* **81**, 113107 (2010).
- [35] R. James and C. R. A. Catlow, *J. Phys. Colloques* **38**, C7-32 (1977).
- [36] D. Adler, *Rev. Mod. Phys.* **40**, 714 (1968).